Power System Technology
ISSN:1000-3673

Received: 16-01-2024 *Revised: 12-02-2024* *Accepted: 07-03-2024*

An Enhanced MPPT Control for PV with Grid Connected EV Charging System

[1] Immanuvel Bright E, [2]Ganesh R, [3]Janani P, [4]Pavithra A P

[1]Assistant Professor, [2]UG Student, [3]UG Student, [4]UG Student

[1]Department of EEE, [2]Department of EEE, [3]Department of EEE, [4]Department of EEE

1Erode Sengunthar Engineering College, Perundurai, Erode, Tamil Nadu, India

Abstract. Due to the rising demand for energy, there is a need to find a different source to address the impending energy crisis, which is most likely accomplished by using gridsynchronized electric vehicles (EV). The integration of multiple EV with grid affects the entire Power system causing imbalance in supply-demand, Voltage and frequency. To minimize these issues we add solar Power in this integration. One of the smart grid's technological developments that enables the transfer of energy between EVs and the grid is called vehicle to grid (V2G) technology. In order to lessen the strain on the grid's voltage and current and to speed up charging, this project uses a Landsman converter along with the Radial Basis Function Neural Network (RBFNN) MPPT technique. A fast convergent approach is Maximum Power Point Tracking (MPPT) using RBFNN. In this work, the Voltage is either boosted or decreased using a Landsman converter. Using a PI controller, the converter's gating circuit is created. If the EV is at rest for long time, the battery gets discharged through the Boost mode and when the EV needs charging, the battery gets charged by the grid through the Buck mode. The excess DC Voltage from PV/ DC Voltage from EV is fed to grid through single phase Voltage source inverter (VSI) and vice versa. The projected plan is authenticated through reproduction using MATLAB. The comparison of the converters shows the greater efficiency of Landsman Converter as 92.3%.

Keywords: EV, V2G, RBFNN, MPPT and VSI.

1 Introduction

Recent trends have shown that electric vehicles (EV) have a number of Power quality problems; therefore, fuel cells (FC) are seen to be the best option for incorporating EV technology to improve performance. A fuel cell electric vehicle is a form of EV that Powers its on-board electric motor using a fuel cell in conjunction with a tiny battery or super-capacitor [1, 2]. However, the Power generated by the FC system is considerably less and insufficient to propel the EV. To provide the required Power, another energy source that has high Voltage gain and good conversion efficiency is therefore needed [3].

When the duty cycle is high, this causes a number of concerns, including reverse recovery problems, Voltage spikes, and shorter lifespan. For FC-based EV propulsion, high switching

Power System Technology
ISSN:1000-3673
Received: 16-01-2024 Revised: 12-02-2024 Accepted: 07-03-2024

frequency and Voltage gain are crucial. As a result, the high-gain converter (HGC) presented in this study uses an upgraded radial basis function (RBF) to increase the system's Voltage gain and conversion efficiency [4, 5]. The fast recursive algorithm (FRA) technique was used to remove superfluous hidden-layer neurons from the RBF neural model [6]. The enhanced RBF method increases the conversion ratio of the HGC without altering the duty cycle value by lowering the Voltage stress and input Current ripple on the Power semiconductor devices [7, 8].

The quantity of knobs in the concealed coating affects how the RBF design is presented. Because of this, the creation of RBF is seen as an issue of optimization that is affected by weight and hidden layer nodes [9, 10]. To increase the vehicle's speed, is used to produce a focused and condensed RBF. The nodes in the hidden layer are identified using improved RBF which gives the output hidden layer node a full impact. In wind systems with variable rotational speeds, the rotational rates are controlled to maximize the power produced by the wind [11]. A crucial element of the wind power system's best performance is MPPT, often known as the hunt for the peak Power state. Effective reactive Power management is equally important to finding the most Power feasible [12].

The generator-side converter benchmarking velocity parameters are easily altered using a single ANN-based technique. The MPPT algorithm, which is based on optimal relationships, determines the dc Voltage reference amounts for the grid side converter. Without using an anemometer, the techniques can estimate wind speed and compute the system parameters [13, 14]. The PI controllers manage the modulations directories of the converting to maximize system performance since there is a mismatch between the desired and actual values for speed and dc voltage, respectively. The generator, drive train, and converter subsystems were all painstakingly and realistically modelled before the MPPT procedures were validated using an everlasting lodestone synchronous producer. By using a Voltage follower strategy to save the DC link Power constant, the EV charger arrangement with Landsman converter is intended to provide an inherent PF improvement at the AC mains. At the Landsman converter's output, a flyback converter receives Power from this constant DC Voltage [15].

The Contribution of the paper are listed as follow:

- Utilize Radial Basis Function (RBFNN) MPPT to get the most Power out of your PV system. Utilize RBFNN MPPT to speed up convergence.
- To achieve a great Power improvement using the Landsman Converter. Using a Landsman converter will lessen the Voltage and Current stress on the grid side.

2 Proposed System Description

In this effort, an EV charging system based on RBFNN is proposed. The system functions in both Vehicle to Grid (V2G) and Grid to Vehicle (G2V) modes when charging is required. It is made up of a PV system, a low Voltage DC bus, a medium Voltage AC grid, and an EV battery. Because the PV system's production is sporadic in nature, a converter is needed to increase it.

Power System Technology
ISSN:1000-3673
Received: 16-01-2024 Revised: 12-02-2024 Accepted: 07-03-2024

In order to increase Voltage gain while reducing losses and increasing efficiency, this system incorporates a Landsman converter.

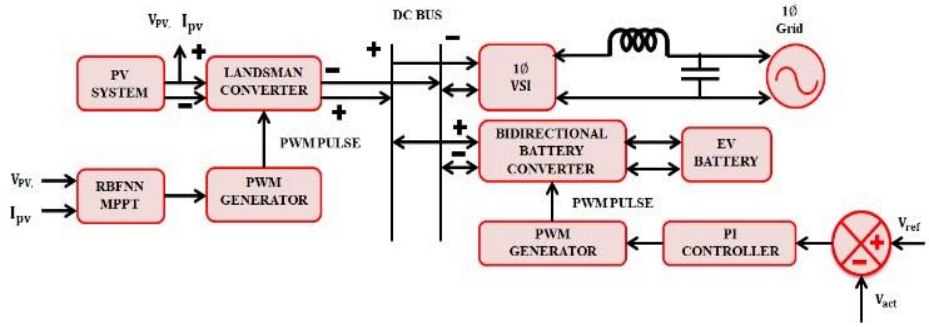

Fig. 1. Proposed Block Diagram

The MPPT algorithm is used in this system by the Landsman converter to get the most Power possible out of the PV system. The output of the planned converter is controlled by pulses produced using the recommended RBFNN MPPT method. The LV DC bus receives the boosted DC Voltage from the Landsman converter. Through a bi-directional battery converter, the electric vehicle battery is charged from the LV DC bus. The grid is also employed as a source for EV charging, and 1 VSI, which serves as a rectifier, transforms MV AC grid Voltage into LV DC. Through 1 VSI, excess energy from PV and energy from vehicles at rest are sent to the grid.

3 Proposed Structure Modelling

3.1 PV System

A semiconductor transistor that has been exposed to light is what makes up a solar cell. Not enough of the solar production's fluctuating energetic atoms are caught at the p-n contact. Compared to band gap, this sector employs the highest energy rays. A single diode is used to construct comparable devices that are frequently employed to simulate PV cells, which strikes a better balance between precision and convenience. Figure 2 presents the corresponding scheme.

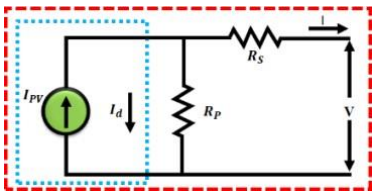

Fig. 2. Circuit of PV cell

The V-I characteristic equation is given by,

Power System Technology
ISSN:1000-3673
Received: 16-01-2024 Revised: 12-02-2024 Accepted: 07-03-2024

$$Iout = ISh - Isat\ [exp\ (V\underline{out}+VIt\underline{outh}\ .R\underline{s}) - 1] - (V\underline{out}+RIs\underline{outh}\ .R\underline{s}) \quad (1)$$

Thus, the PV organization description is made, and (1) is used to evaluate the yield Power and effort Voltage.

3.2 Landsman Converter

The circuit diagram below shows the unnecessary active and passive parts of the Landsman converter. Additionally, this converter can conduct buck and boost operations, although the output is inverted.

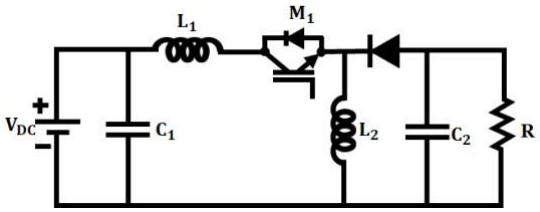

Fig. 3. Landsman Converter

Mode 1: The capacitors C1, L1, and L2 are charged by the Voltage Vdc when the switch is in this mode. D develops a reverse bias.

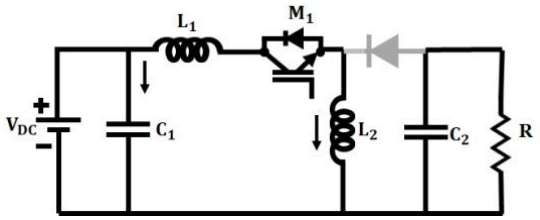

Fig. 3 (a) Mode 1

Mode 2: When switched is turned off, D conducts and becomes forward biased. At this point, the energy stored in passive aspects is used to energize C2 and the load.

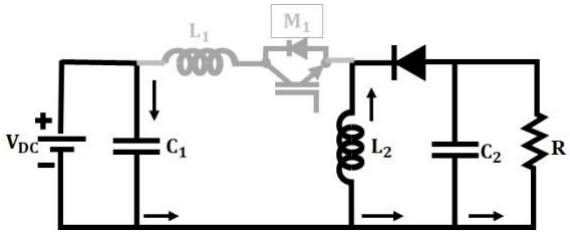

Fig. 3 (b) Mode 2

Power System Technology
ISSN:1000-3673
Received: 16-01-2024 Revised: 12-02-2024 Accepted: 07-03-2024

3.3 Single Phase VSI

The impact of the DC input is converted into a single point of AC output influence at a certain Voltage and intensity using a particular type of DC to AC converter known as a single stage inverter. Existing base inverters and VSI are the two fundamental variances. Continuous DC input Power is converted into AC output Power utilizing VSI. The output Current diverges according to the freight impedance, and the irreversible Power of this inverter keeps breaking.

3.4 RBFNN Based MPPT

Utilizing radial basis purpose neural network, a unique supervisor with an adaptive following approach is produced to boost MPPT efficacy. It has been used in a variety of industries, including wind and electricity forecasts. In this instance, the RBFNN is recommended to approach the optimal torque. For this control strategy, the well characteristics of the wind turbines are not required. As a result of its quick adaption time, which improves MPPT performance, it could follow the dynamic wind swiftly.

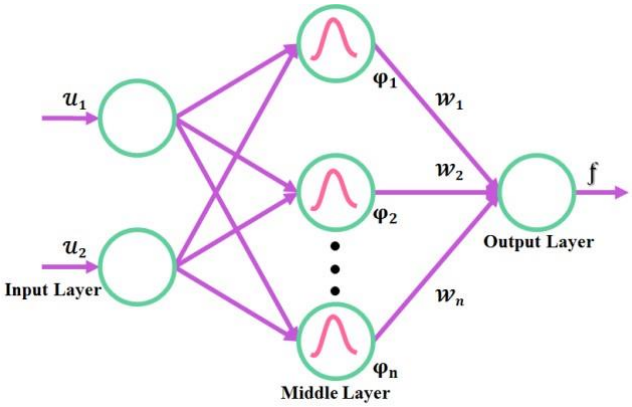

Fig. 4. RBFNN based MPPT

This study provides a torque and pitch controller-equipped wind turbine system with an MPPT switch. The only prerequisite for the RBFNN-based referenced torque controller comparable ideal value is the best TSR. Figure 4 depicts the RBFNN's layer structure.

$$\emptyset_1(u_1, u_2) = exp(-\frac{u-c_i}{2}) \quad (2)$$
$$2\delta$$

$$f = \sum \emptyset_1 w_i \quad (3)$$

By adjusting the weightw_i, rendering to single rules, the output was changed. The rule is often chosen using the gradient descent approach.

Power System Technology
ISSN:1000-3673
Received: 16-01-2024 Revised: 12-02-2024 Accepted: 07-03-2024

4 Results and Discussion

The intended work is carried out exactly as planned in MATLAB, and the resultant Waveform flow is detailed below:

Table 1. Parameter Specifications

Parameters	Values
L_1 and L_2	1.5mH
Capacitance (C_1)	$4.7\mu F$
Capacitance (C_2)	$2.2\mu F$
R	100Ω
Mosfet Switch	10KHz

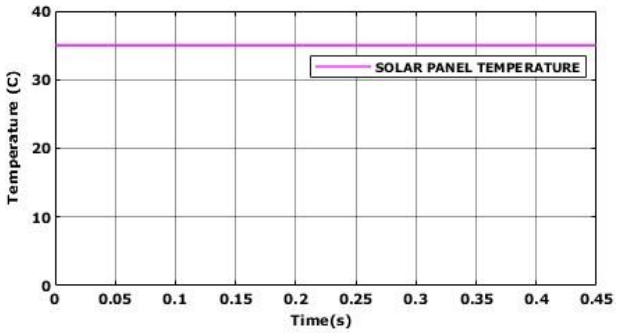

Fig. 5. Solar Panel temperature Waveform

The board's temperature undulation is maintained at 35°C and is shown in Figure 5 to be constant.

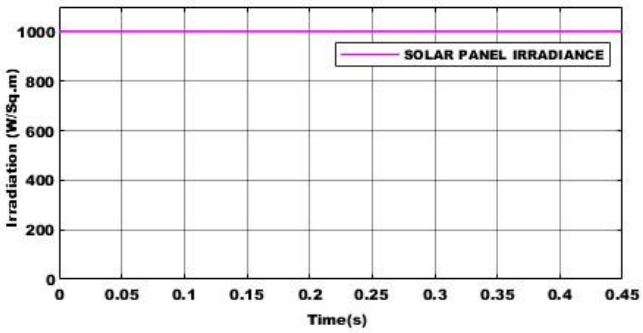

Fig. 6. Solar Panel Irradiance Wave

Figure 6 demonstrates that the solar panel's irradiation waveform remains a constant 1000W/Sq.m.

Power System Technology
ISSN:1000-3673
Received: 16-01-2024 Revised: 12-02-2024 Accepted: 07-03-2024

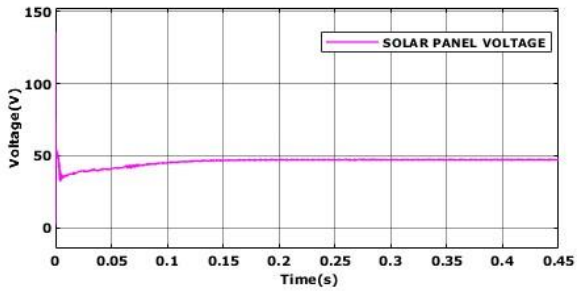

Fig. 7. Solar Panel Voltage Waveform

For 0.02 seconds, the undulation is maintained at 140V. After 0.3 seconds, the voltage waveform drops to 50V and then remains continuous.

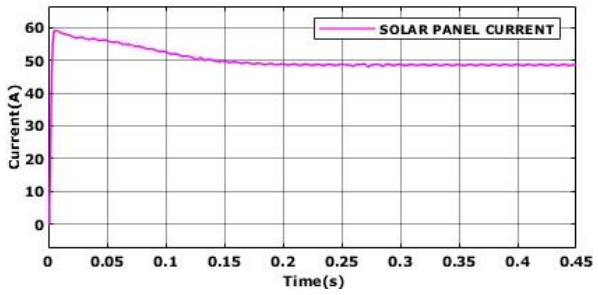

Fig. 8. PV Current Wave

An Undulation increases from 0 A to 60 an over a 0.01 second period. Following a 50A waveform reduction for 0.15 seconds, the waveform remains steady.

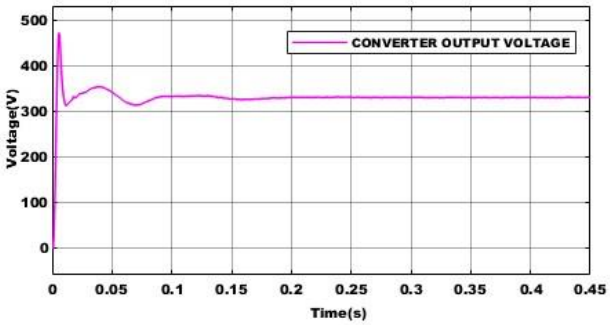

Fig. 9. Converter output Voltage

The converter maintains its 390V output voltage for up to 0.01 seconds. The voltage waveform lowers to 320V after 0.01s and maintains constant there for the next 0.1s.

Power System Technology
ISSN:1000-3673
Received: 16-01-2024 Revised: 12-02-2024 Accepted: 07-03-2024

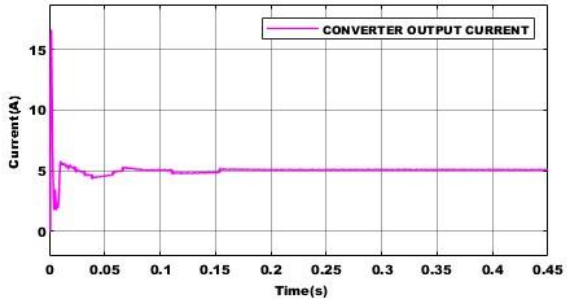

Fig.10. Converter produce Current Wave

The waveform of the converter's output current is held at 17A for 0.01s. The current waveform dropped to 5A and stayed there for 0.02 seconds after 0.01 seconds.

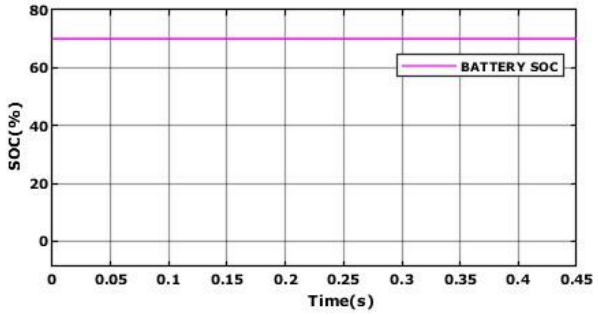

Fig. 11. Battery SOC Waveform

The battery's state of charge waveform for output power is maintained at 70% in Figure 11, which is a constant value.

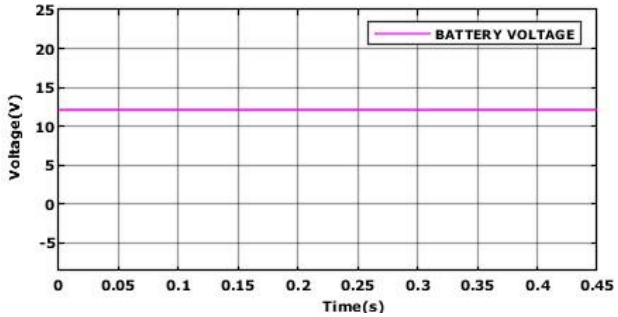

Fig. 12. Battery Voltage Waveform

The battery voltage waveform seen in Figure 12 needs to stay constant at 12.5V.

Power System Technology
ISSN:1000-3673
Received: 16-01-2024 Revised: 12-02-2024 Accepted: 07-03-2024

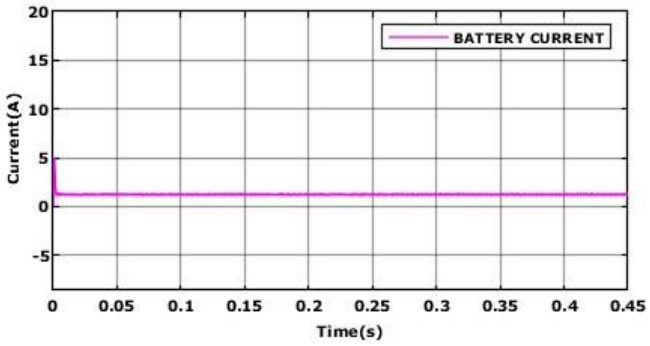

Fig. 13. Battery Current Waveform

Figure 13 displays the waveform of the battery's current. It keeps the fixed value at 0A.

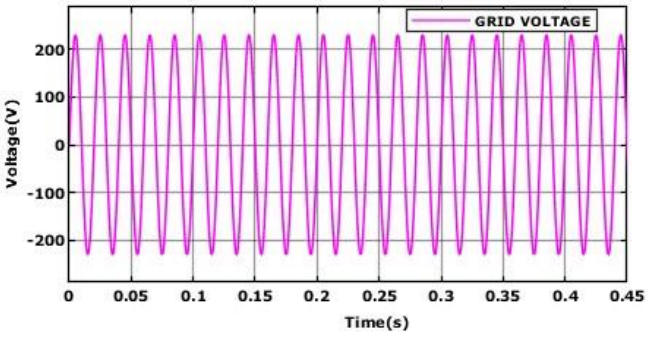

Fig. 14. Grid Voltage Waveform

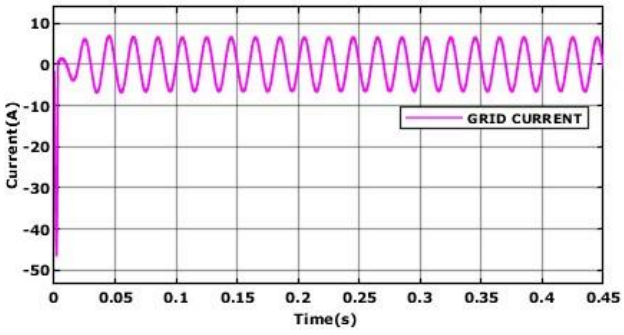

Fig. 15. Grid Current Waveform

The grid's 200V output voltage, which is maintained steady and free of fluctuations, is shown in Figure 14. The grid's output current is constant and equals 0 A, matching the output voltage, as shown in Figure 15.

Power System Technology
ISSN:1000-3673
Received: 16-01-2024 Revised: 12-02-2024 Accepted: 07-03-2024

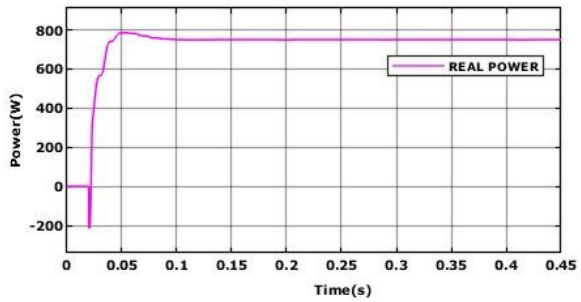

Fig. 16. Real Power Waveform

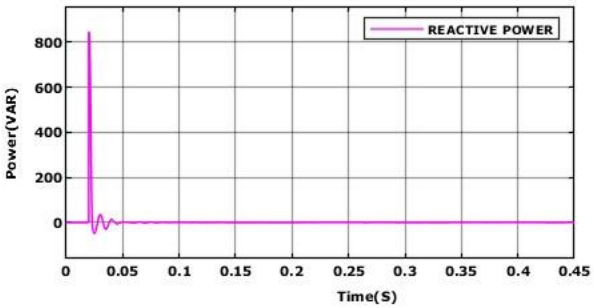

Fig. 17. Reactive Power Waveform

The reactive power has increased from 0 and decreased to 0VAR and has remained constant, as indicated in Figures 16 and 17, whereas the real power of the grid has a high value of 700W.

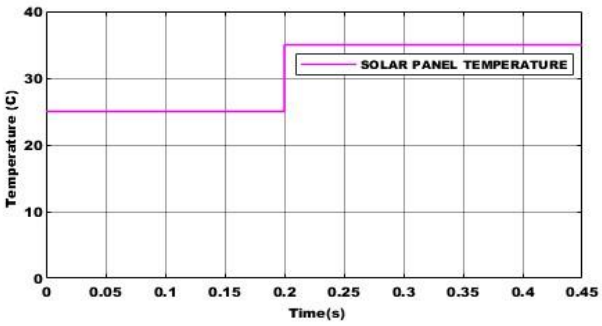

Fig. 18. Solar Panel Temperature Waveform

The temperature waveform of the solar panel is held steady at 25 °C for 0.2 seconds. The temperature waveform reaches 35°C after 0.2s and then stays there.

Power System Technology
ISSN:1000-3673
Received: 16-01-2024 Revised: 12-02-2024 Accepted: 07-03-2024

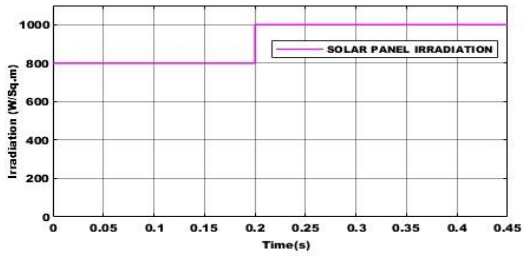

Fig. 19. Solar Panel Irradiation Waveform

The photovoltaic array keeps its irradiation waveforms at 800W/Sq.m for up to 0.2 seconds. The irradiation distribution grows to 1000W/Sq.m after 0.2s and then remains consistent.

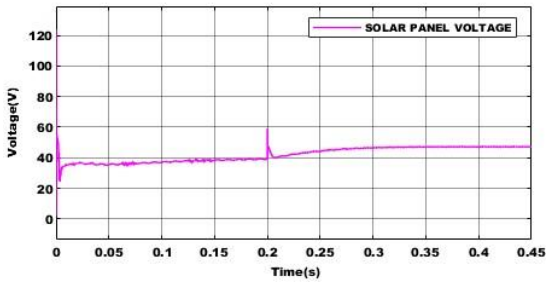

Fig. 20. Solar Panel Voltage Waveform

The solar panel's irradiation waveforms is held steady at 800W/Sq.m for up to 0.2 seconds. After 0.2 seconds, the ionizing pattern grows to 1000W/Sq.m and then remains constant.

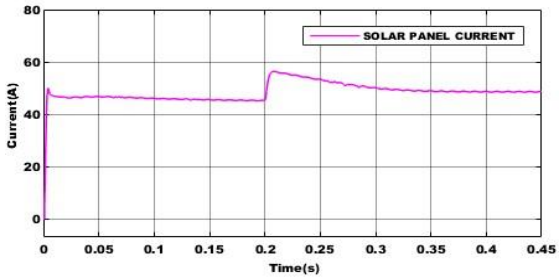

Fig. 21. Solar Panel Current Waveform

For 0.02 seconds, the solar panel's current waveforms is maintained at 50A. After 0.02s, the sine wave rises to 59V and stays that way for the following 0.2s.

Power System Technology
ISSN:1000-3673
Received: 16-01-2024 Revised: 12-02-2024 Accepted: 07-03-2024

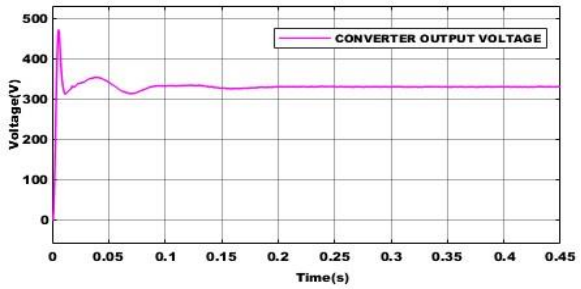

Fig. 22. Converter output Voltage Waveform

For 0.01s, waveform of the converter is maintained at 490V. After 0.01s, the voltage waveform dips to 300V and remains stable there for the following 0.1s.

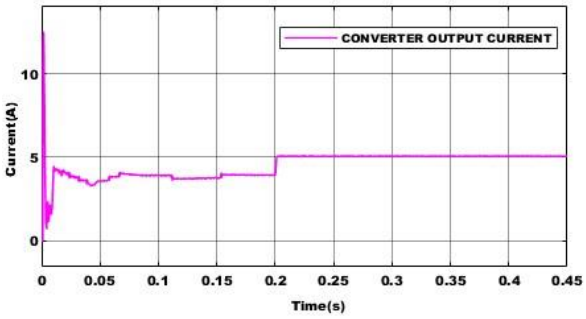

Fig. 23. Converter output Current Waveform

Fig. 23 shows the waveform of the converter's yield current, which falls from a value of 12A after maintaining a constant value of 5A.

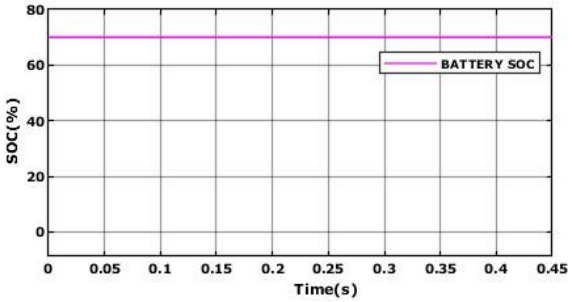

Fig. 24. Battery SOC Waveform

Figure 24 shows the battery's SOC waveform at a constant value for 70% of the time.

Power System Technology
ISSN:1000-3673
Received: 16-01-2024 Revised: 12-02-2024 Accepted: 07-03-2024

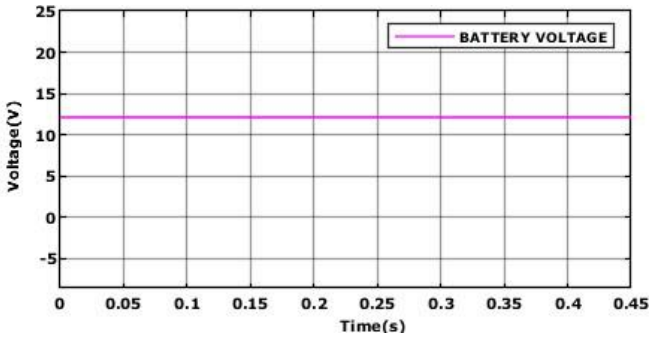

Fig. 25. Battery Voltage Waveform

The battery voltage waveform shown in Figure 25 is kept at 12.5V.

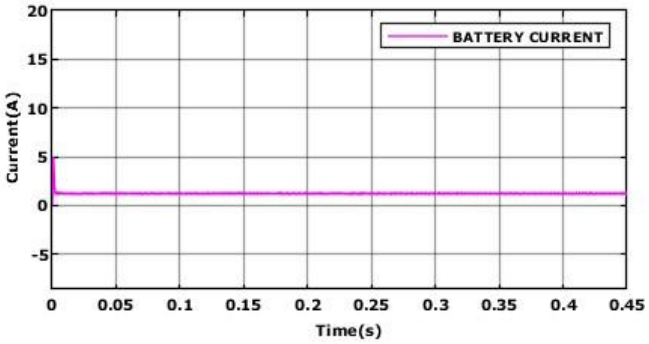

Fig. 26. Battery Current Waveform

The battery current waveform, which is kept at 2A, is shown in Figure 26.

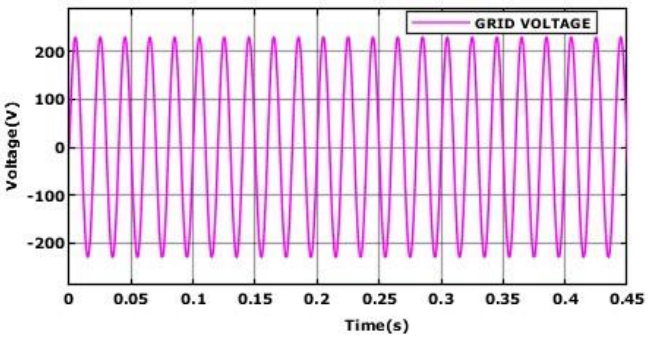

Fig. 27. Grid Voltage Waveform

As can be seen in Figure 27 the Grid voltage waveform maintains a steady value of 200V.

Power System Technology
ISSN:1000-3673
Received: 16-01-2024 Revised: 12-02-2024 Accepted: 07-03-2024

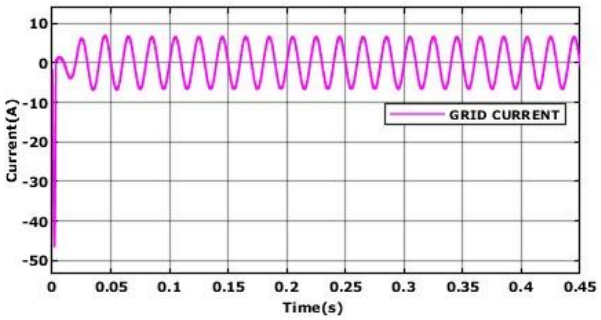

Fig. 28. Grid Current Waveform

That grid as can be seen in Figure 28, the current waveform starts off negative and then grows to a constant value of 0A.

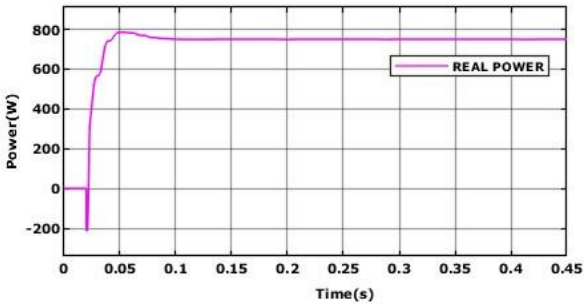

Fig. 29. Real Power Waveform

The actual power waveform is depicted in Figure 29 it starts off at 0W and decreases before increasing from an adverse number and remaining constant at 790W.

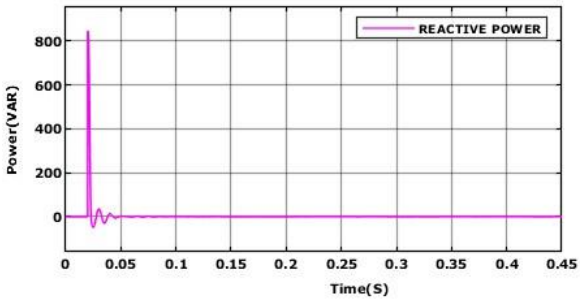

Fig. 30. Reactive Power Waveform

Figure 30 depicts the reactive power waveform as it grows from zero to 820 VAR before dropping to a constant value of 0 VAR.
Figure 31 shows the values for the Efficiency Comparison of the Converters, which are stated as 87%, 88.5%, 89%, 90.2%, and 92.3% for the boost, Cuk, Sepic, and Landsman Converters, respectively.

Power System Technology
ISSN:1000-3673
Received: 16-01-2024 Revised: 12-02-2024 Accepted: 07-03-2024

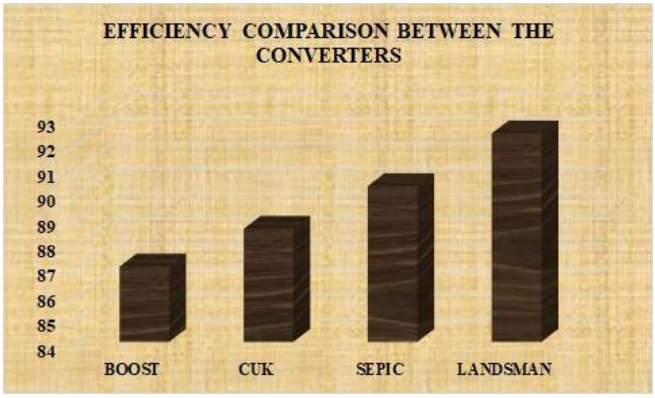

Fig. 31. Comparison between the Converters

5 Conclusion

A grid-connected EV charging system is suggested in this project. This endeavor integrates the Landsman converter with the RBFNN MPPT approach to reduce the voltage and current stress on the grid side and speed up charging. A method that rapidly converges is RBFNN MPPT. In this study, the voltage is changed in both directions using a bidirectional DC-DC converter. The filtering sequence of the converter is designed using a PI controller. The Buck mode allows the grid to recharge the battery when the EV is in need of charging. The battery is depleted through the Boost mode if the EV is left stationary for a lengthy period of time. The excess DC voltage produced by solar panels and electric vehicles is transmitted to the grid using a single phase VSI. The proposed method is validated using MATLAB simulation. When the converters are compared, Landsman Converter has a higher efficiency of 92.3%.

References

1. Reddy, B. R. S., Reddy, V. V., Vijaya Kumar, M.: Modelling and analysis of DC-DC converters with AI based MPP tracking approaches for grid-tied PV-fuel cell system. Electric Power Systems Research **216**, 109053 (2023).
2. Rao, C. V., David Amar Raj, R., Anil Naik, K.: A novel hybrid image processing-based reconfiguration with RBF neural network MPPT approach for improving global maximum power and effective tracking of PV system. International Journal of Circuit Theory and Applications (2023).
3. Ganti, P. K., Naik, H., Barada, M. K.: Hybrid TSA-RBFNN based approach for MPPT of the solar PV panel under the effects of tilt angles variations and environmental effects. International Journal of Energy Research **45**(14), 20104-20131 (2021).
4. Priyadarshi, N., Sanjeevikumar, P., Bhaskar, M. S., Azam, F., BM Taha, I., Hussien, M. G.: An adaptive TS-fuzzy model based RBF neural network learning for grid integrated photovoltaic applications. IET Renewable Power Generation **16**(14), 3149-3160 (2022).

Power System Technology
ISSN:1000-3673
Received: 16-01-2024 Revised: 12-02-2024 Accepted: 07-03-2024

5. Rahman, M. M. A., Rahim, A. H. M. A.: Design and testing of an MPPT algorithm using an intelligent RBF neural network and optimum relation based strategy. In 2020 IEEE Region 10 Symposium (TENSYMP), 1245-1248 (2020).
6. Sitharthan, R., Karthikeyan, M., Shanmuga Sundar, D., Rajasekaran, S.: Adaptive hybrid intelligent MPPT controller to approximate effectual wind speed and optimal rotor speed of variable speed wind turbine. ISA transactions **96**, 479-489 (2020).
7. Nguyen, T. N. A., Pham, D. C., Luu, H. M., Thanh, N. H. C.: Combined RBFN based MPPT and d-axis stator current control for permanent magnet synchronous generators. International Journal of Power Electronics and Drive Systems **12**(4), 2459 (2021).
8. Hamdi, H., Regaya, C. B., Zaafouri, A.: Real-time study of a photovoltaic system with boost converter using the PSO-RBF neural network algorithms in a MyRio controller. Solar energy **183**, 1-16 (2019).
9. Jing, Z., Ning, L., Jiabin, X., Shengfang, Z., Yan, X.: Novel MPPT method based on large variance GA-RBF. The Journal of Engineering 16, 3365-3370 (2019).
10. Chandra, S., Gaur, P., Pathak, D.: Radial basis function neural network based maximum power point tracking for photovoltaic brushless DC motor connected water pumping system. Computers & Electrical Engineering **86**, 106730 (2020).
11. Chandra, S., Gaur, P.: Radial basis function neural network technique for efficient maximum power point tracking in solar photo-voltaic system. Procedia Computer Science **167**, 23542363 (2020).
12. Zhang, Y., Wang, Y. J., Zhang, Y., Yu, T.: Photovoltaic fuzzy logical control MPPT based on adaptive genetic simulated annealing algorithm-optimized BP neural network. Processes **10**(7), 1411 (2022).
13. Rajesh, P., Shajin, F. H., Cherukupalli, K.: An efficient hybrid tunicate swarm algorithm and radial basis function searching technique for maximum power point tracking in wind energy conversion system. Journal of Engineering, Design and Technology (2021).
14. Rafikiran, S., Devadasu, G., Rajendhar, P., Likhitha, R., Basha, C. H.: Design and implementation of hybrid MPPT controller for FC based EV system with boost DC-DC converter. Journal of Intelligent & Fuzzy Systems Preprint, 1-19 (2022).
15. Ramasamy, K., Ravichandran, C. S.: Optimal design of renewable sources of PV/wind/FC generation for power system reliability and cost using MA-RBFNN approach. International Journal of Energy Research **45**(7), 10946-10962 (2021).